Twin-Directed Deposition of Pt on Pd Icosahedral Nanocrystals for Catalysts with Enhanced Activity and Durability toward Oxygen Reduction

Mingkai Liu, Zhiheng Lyu, Yu Zhang, Ruhui Chen, Minghao Xie, Younan Xia*

Materials. Sodium tetrachloropalladate (Na_2PdCl_4, 98%), potassium tetrachloroplatinate (K_2PtCl_4, 98%), poly(vinyl pyrrolidone) (PVP, MW ≈ 55,000), diethylene glycol (DEG), L–ascorbic acid (AA), and potassium bromide (KBr) were obtained from Sigma–Aldrich. Deionized (DI) water with a resistivity of 18.2 MΩ·cm at room temperature was used in all the experiments.

Synthesis of Pd icosahedra. The Pd icosahedra with an average size of 9.5 nm were synthesized according to our previously reported protocol.[1] Typically, 160 mg of PVP was dissolved in 4 mL of DEG in a 20-mL vial by heating at 130 ºC for 10 min under magnetic stirring. Subsequently, 31 mg of Na_2PdCl_4 was dissolved in 2 mL of DEG and the solution was injected into the PVP solution in one shot. This reaction was maintained at 130 ºC for 3 h under magnetic stirring. The solid product was collected by centrifugation, washed once with acetone and twice with water, and dispersed in 6 mL of water for further use.

Synthesis of Pd-Pt great icosahedra. In a standard protocol, 1 mL of the aqueous suspension of Pd icosahedra, 70 mg of PVP, 50 mg of AA, and 4 mL of water were mixed in a 20-mL vial and heated at 30 ºC for 20 min under magnetic stirring. At the same time, 3.5 mg of KBr and 1.5 mg of K_2PtCl_4 were dissolved in 2 mL of water and the solution was added into the vial in one shot. The reaction was maintained at 30 ºC for another 24 h. The solid product was collected by centrifugation, washed once with acetone and twice with water, and dispersed in 2 mL of water.

Characterization. Transmission electron microscopy (TEM) images were taken using a Hitachi HT7700 microscope operated at 120 kV. High-resolution TEM images and energy-dispersive X-ray (EDX) spectroscopy data were acquired on an aberration-corrected Hitachi HD-2700 scanning TEM (STEM) equipped with a Brüker Quantax 400/S–STEM EDX detector at 200 kV. Before imaging, the sample was cleaned in a Hitachi Zone cleaner for 30 min at a pressure setting of 30. X-ray photoelectron spectroscopy (XPS) measurements were conducted using a Thermo Scientific K-Alpha spectrometer with an Al Kα microfused monochromic source.

Preparation of the working electrode. Separately, 5 mg of the Pd-Pt great icosahedra were dispersed in 5 mL of water and 15 mg of carbon support (Vulcan XC-72) was dispersed in 10 mL of water. These two suspensions were then mixed together under sonication at room temperature, followed by sonicating for another 3 h. The carbon-supported catalyst was collected by centrifugation at 15,000 rpm, and then dispersed in 12 mL of acetic acid, treated at 60 °C for 3 h under magnetic stirring to remove excess PVP. The solid was collected by centrifugation and washed with ethanol eight times to further clean the surface. The final product was dried at 70 °C for 2 h. In the following step, 16.4 mg of the catalyst was dispersed in a mixture of 3.98 mL of isopropanol and 20 μL of 5% Nafion under ultrasonication for 1 h. The final concentration of Pt in the as-prepared catalyst was determined to be 0.256 mg·mL^{-1} by inductively coupled plasma mass spectrometry (ICP-MS, NexION 300Q, Perkin-Elmer). 8 μL of the suspension was deposited on a pre-cleaned glassy carbon rotating disk electrode (RDE, 0.196 cm^2 in geometric area, Pine Research Instrumentation) and dried at room temperature. The working electrode was further dried at 60 °C for 1 h in an oven. Commercial Pt/C (20 wt%, Pt nanoparticles on Vulcan XC-72 carbon support; E-TEK) was prepared with the same protocol and used for comparison.

Electrochemical measurements. All the measurements were conducted in a three-electrode system connected to a CHI 600E electrochemical workstation (CH Instruments). A Hydroflex reference electrode (Gaskatel) was used as the reference electrode, a Pt mesh as the counter electrode, and 0.1 M aqueous HClO$_4$ solution as the electrolyte. The cyclic voltammetry (CV) curves were recorded in a N$_2$-saturated 0.1 M HClO$_4$ aqueous solution at a scanning rate of 50 mV·s^{-1} in the potential range of 0.05–1.1 V$_{RHE}$ (RHE: reversible hydrogen electrode). Electrochemical active surface areas (ECSAs) were calculated from the average charges associated with the adsorption of hydrogen from 0.05 to 0.4 V after double-layer correction with a reference value of 210 μC·cm^{-2}.[2] The ORR activity of each sample was investigated by conducting the linear sweep voltammetry (LSV) tests in an O$_2$-saturated 0.1 M HClO$_4$ solution at room temperature at a scanning rate of 10 mV·s^{-1} (rotating speed: 1,600 rpm). The data were corrected by 85% IR drop compensation. The accelerated durability tests (ADTs)

were carried out in the range of 0.6–1.1 V_{RHE} for 5,000 and 10,000 cycles at a scan rate of 100 mV·s^{-1} in O_2-saturated 0.1 M $HClO_4$ solution. The kinetic current was calculated based on the derived Koutecky-Levich equation:

$$j_k = \frac{j_l \times j}{j_l - j}$$

where j_k is the kinetic current, j_l is the diffusion-limiting current, and j is the current experimentally measured at 0.9 V_{RHE}. Mass and specific activities of samples were obtained by normalizing the kinetic current to the amount of loaded Pt and ECSA value, respectively.
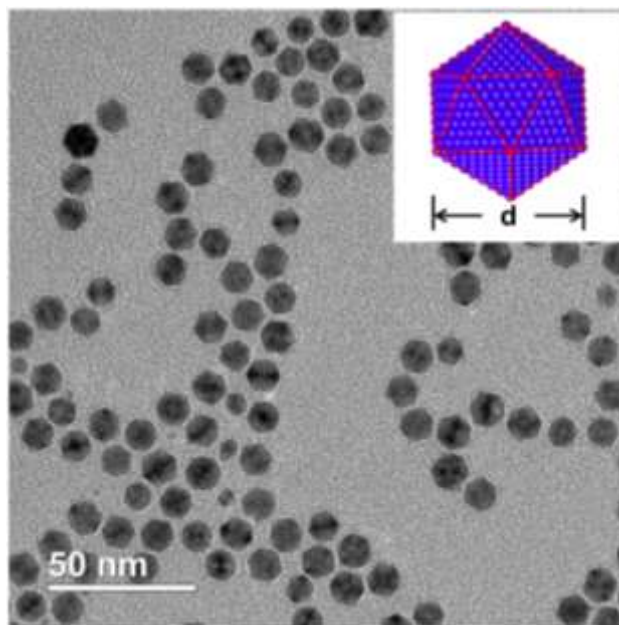
Figure S1. A typical TEM image of the Pd icosahedral seeds, with the inset illustrating the definition of size.
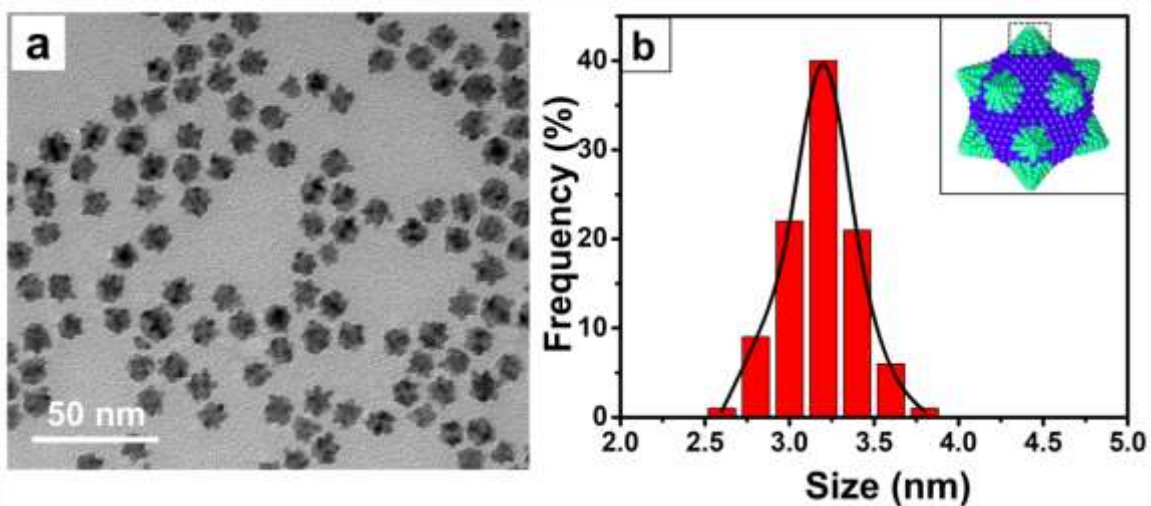
Figure S2. (a) TEM image of the as-synthesized Pd-Pt great icosahedra and (b) the size distribution of the multiply-twinned Pt dots (see the inset for a model, with the size of the dot being defined by its height).
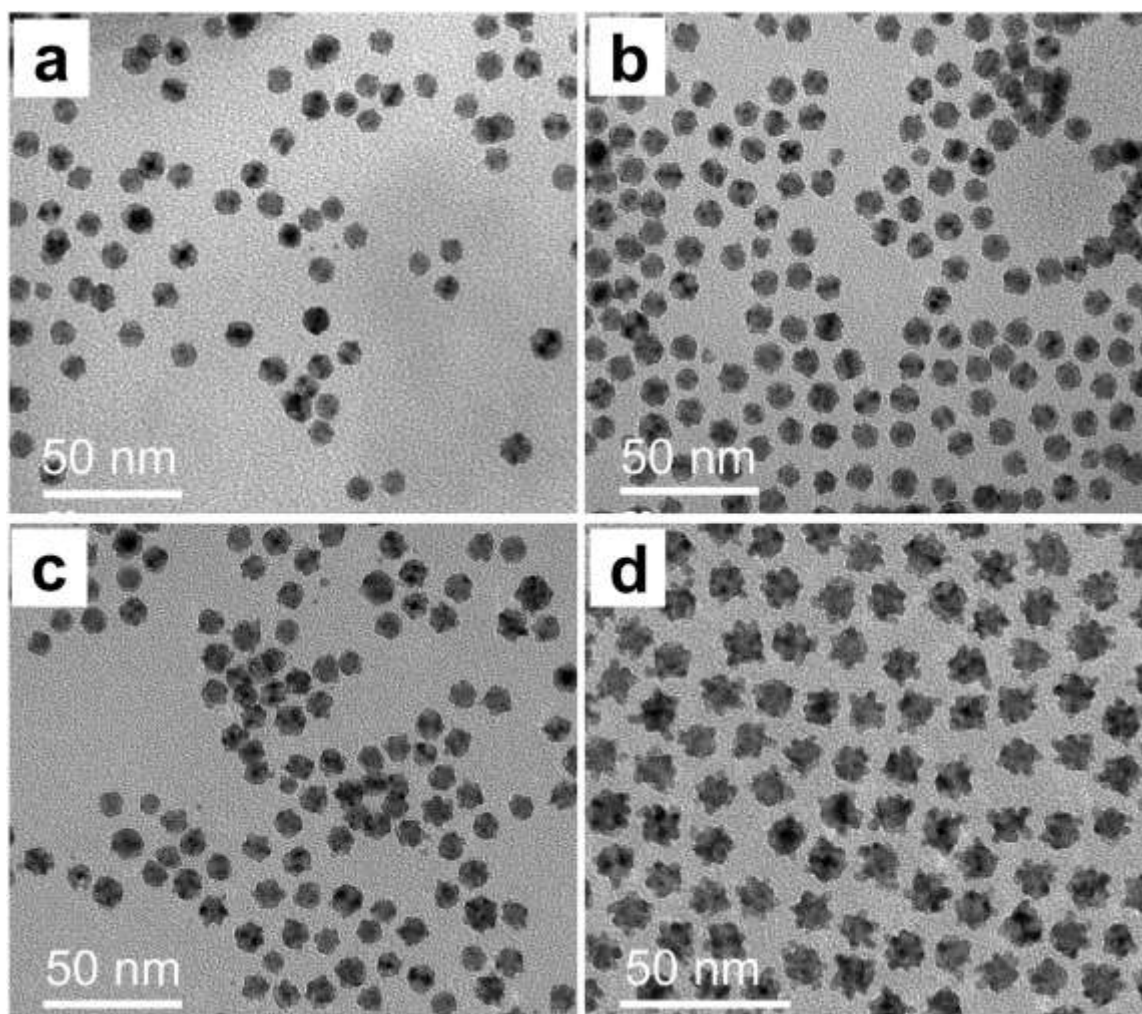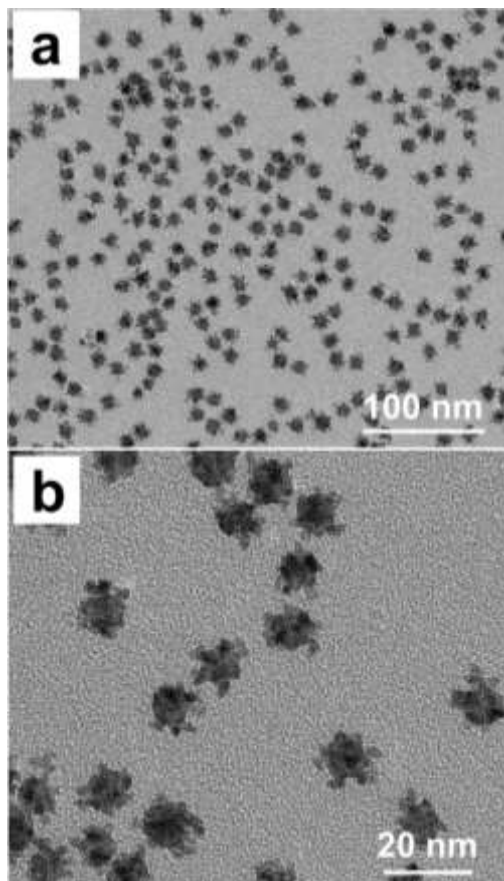
Figure S3. TEM images of the Pd-Pt bimetallic nanocrystals prepared using the standard protocol except for the variation in the amount of K_2PtCl_4: (a) 0.2, (b) 0.5, (c) 1.0, and (d) 2.0 mg, respectively.
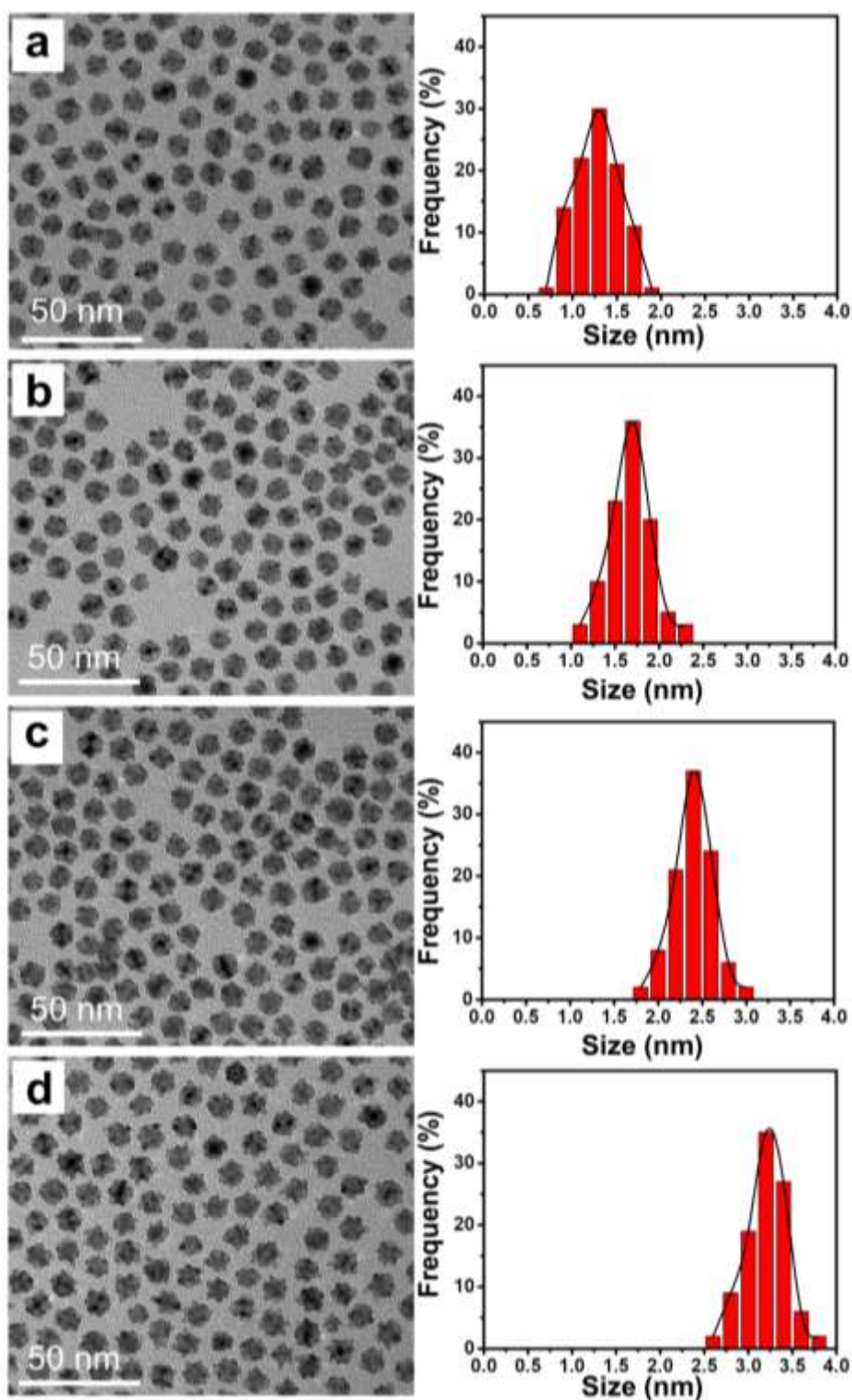
Figure S4. TEM images of the Pd-Pt bimetallic nanocrystals prepared using the standard protocol except for the variation in reaction time: (a) 6, (b) 12, (c) 18, and (d) 24 h, respectively. The plots in the right column represent the corresponding size distributions of the Pt dots deposited on the Pd icosahedral seeds.

Figure S5. TEM images, at two different magnifications, of the Pd-Pt bimetallic nanocrystals prepared using the standard protocol except for the absence of Br⁻.
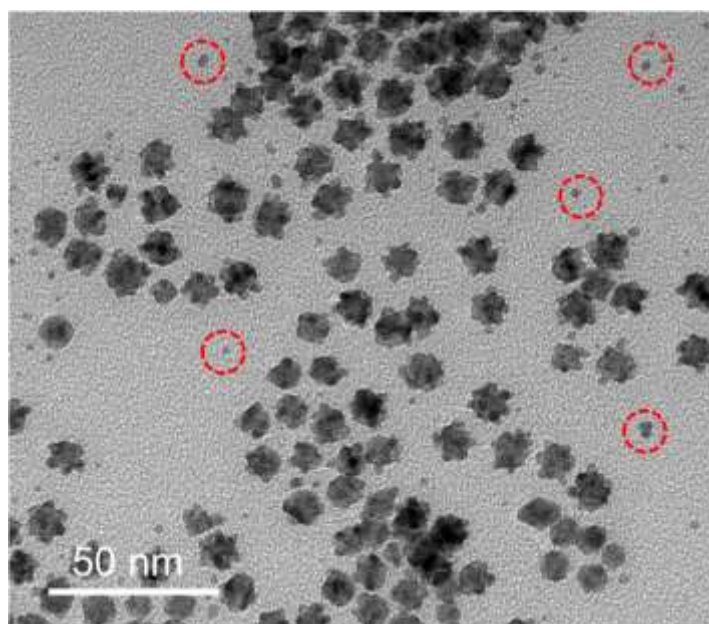
Figure S6. TEM image of the Pd-Pt nanocrystals prepared using the standard protocol except for raising the reaction temperature to 90 ºC. The circles indicate the Pt nanoparticles formed through homogeneous nucleation.
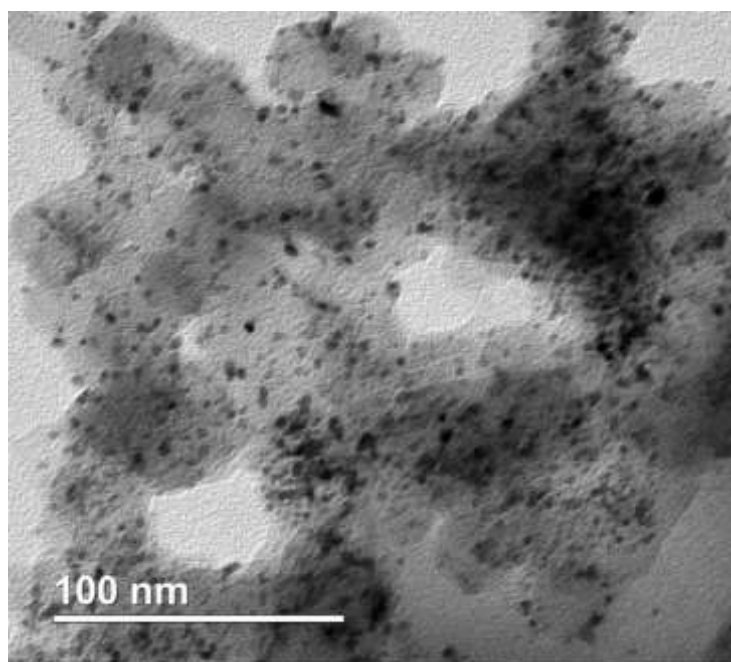
Figure S7. TEM image of the commercial Pt/C catalyst.
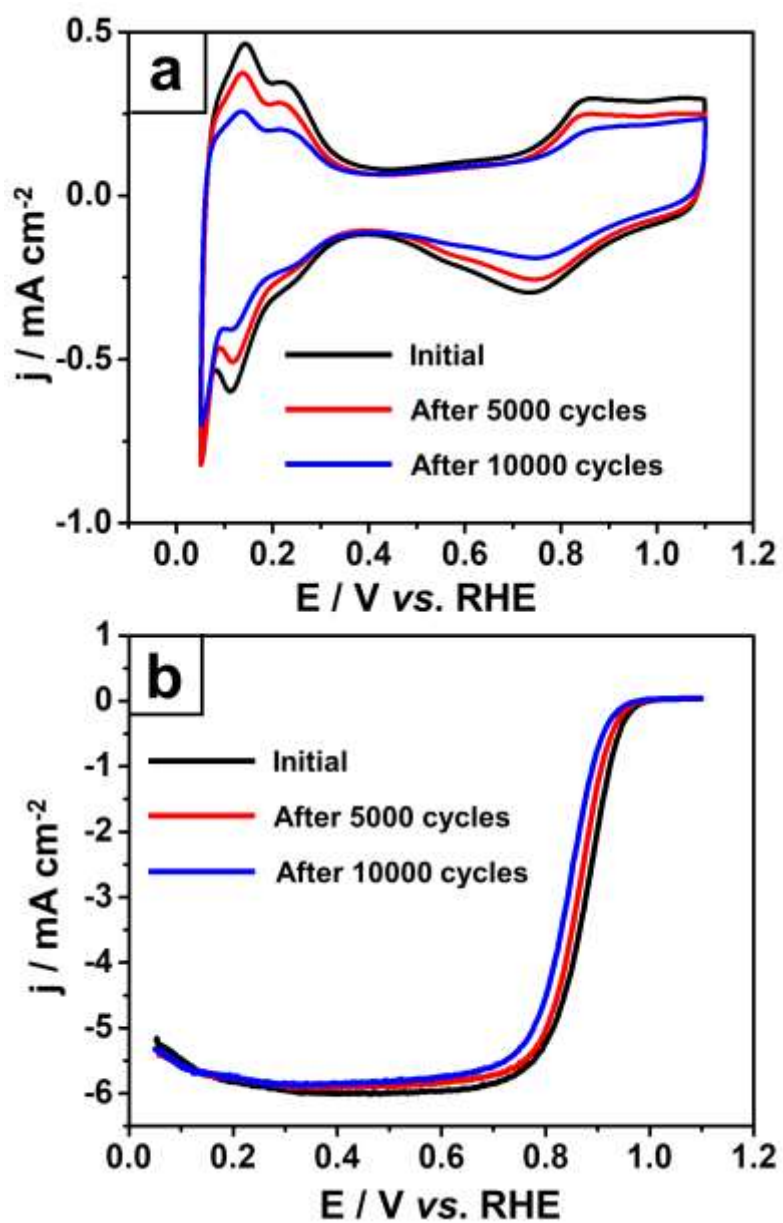
Figure S8. (a) CV and (b) oxygen reduction polarization curves recorded from the commercial Pt/C catalyst before and after different cycles of ADT. The currents were normalized to the geometric area of RDE.
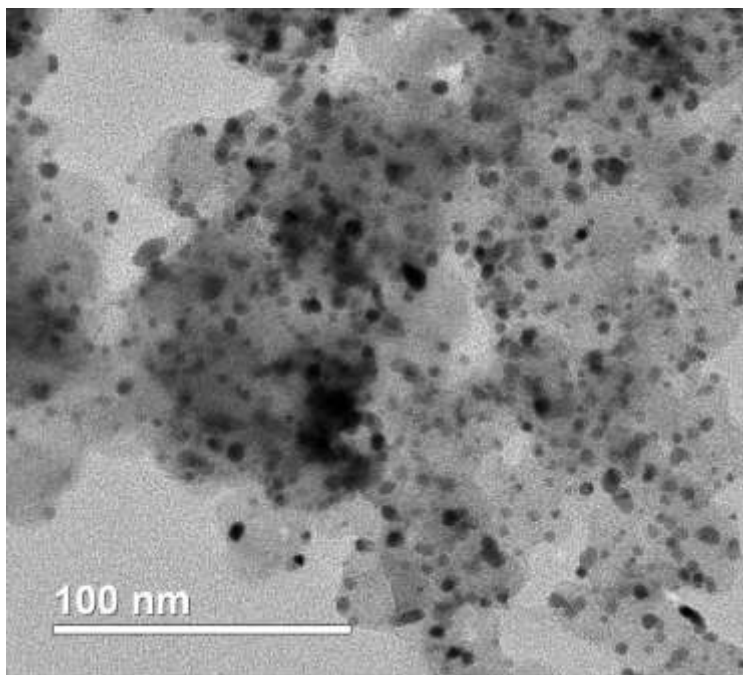
Figure S9. TEM images of the commercial Pt/C catalyst after 10000 cycles of ADT.

Table S1. ECSAs, half-wave potentials, mass activities, and specific activities of Pd-Pt great icosahedra and commercial Pt/C before and after different cycles of ADT.

Sample	Cycles	ECSA $(m^2\ g^{-1}_{Pt})$	Half-wave potential (V)	Mass activity $(A\ mg^{-1}_{Pt})$	Specific Activity $(mA\ cm^{-2})$
Pd-Pt great icosahedra	initial	124.1	0.92	1.23	0.99
	5000	107.3	0.91	1.18	1.10
	10000	106.8	0.91	1.09	1.02
Commercial Pt/C	initial	71.2	0.87	0.15	0.22
	5000	47.1	0.85	0.10	0.21
	10000	39.5	0.84	0.07	0.18

Table S2. Comparative evaluation of electrocatalytic properties of the Pd-Pt great icosahedra with reported state-of-the-art Pd/Pt-based electrocatalysts.

Sample	ECSA $(m^2\ g^{-1}_{Pt})$	Mass activity $(A\ mg^{-1}_{Pt})$	Specific activity $(mA\ cm^{-2})$	Ref.
Pd-Pt great icosahedra	124.1	1.23	0.99	This work
Pd@Pt core−shell concave decahedra	95.9	1.60	1.66	3
Pd@Pt octahedra	70	1.05	1.51	4
Pt-Pd concave nanocubes	45.2	0.87	1.93	5
Pd@Pt core−shell concave nanocubes	61	0.84	1.38	6
Pd@Pt core−shell nanowires	202.5	0.81	0.4	7
Pd-Pt octahedral nanocages	40.3	0.76	1.9	8
Pd@Pt$_{1L}$ octahedra	74.3	0.75	1.01	9
Pd@Pt core–shell nanoparticles	48.82	0.58	0.44	10
Pt-Pd popcorns	47.4	0.57	0.52	11
PdPt bimetallic nanocrystals	49.2	0.52	1.89	12
Pd@Pt$_{2–3L}$ octahedra	53.6	0.49	0.91	13
Pt-Pd nanodendrites	92.4	0.40	0.44	14
Pd@Pt$_{4.5L}$ core-shell icosahedron	46.0	0.39	0.83	15
Pt@Pd core−shell icosahedra	38.8	0.29	0.74	16
Pd@Pt core−shell nanodots	84.38	0.20	0.24	17

References

(1) Yang, T. H.; Zhou, S.; Gilroy, K. D.; Figueroa-Cosme, L.; Lee, Y. H.; Wu, J. M.; Xia, Y., Autocatalytic Surface Reduction and Its Role in Controlling Seed-mediated Growth of Colloidal Metal Nanocrystals. *Proc. Natl. Acad. Sci. U. S. A.* **2017**, *114*, 13619−13624.

(2) Lee, C.-T.; Wang, H.; Zhao, M.; Yang, T.-H.; Vara, M.; Xia, Y., One-Pot Synthesis of Pd@PtnL Core-Shell Icosahedral Nanocrystals in High Throughput through a Quantitative Analysis of the Reduction Kinetics. *Chem. Eur. J.* **2019**, *25*, 5322−5329.

(3) Wang, X.; Vara, M.; Luo, M.; Huang, H.; Ruditskiy, A.; Park, J.; Bao, S.; Liu, J.; Howe, J.; Chi, M.; Xie, Z.; Xia, Y., Pd@Pt Core–Shell Concave Decahedra: A Class of Catalysts for the Oxygen Reduction Reaction with Enhanced Activity and Durability. *J. Am. Chem. Soc.* **2015**, *137*, 15036−15042.

(4) Zhou, M.; Wang, H.; Vara, M.; Hood, Z. D.; Luo, M.; Yang, T.-H.; Bao, S.; Chi, M.; Xiao, P.; Zhang, Y.; Xia, Y., Quantitative Analysis of the Reduction Kinetics Responsible for the One-Pot Synthesis of Pd–Pt Bimetallic Nanocrystals with Different Structures. *J. Am. Chem. Soc.* **2016,** *138*, 12263-12270.

(5) Wu, R.; Tsiakaras, P.; Shen, P. K., Facile Synthesis of Bimetallic Pt-Pd Symmetry-broken Concave Nanocubes and Their Enhanced Activity toward Oxygen Reduction Reaction. *Appl. Catal. B Environ.* **2019**, *251*, 49−56.

(6) Lee, S. R.; Park, J.; Gilroy, K. D.; Yang, X.; Figueroa-Cosme, L.; Ding, Y.; Xia, Y., Palladium@Platinum Concave Nanocubes with Enhanced Catalytic Activity toward Oxygen Reduction. *ChemCatChem* **2016**, *8*, 3082−3088.

(7) Li, H.-H.; Ma, S.-Y.; Fu, Q.-Q.; Liu, X.-J.; Wu, L.; Yu, S.-H., Scalable Bromide-Triggered Synthesis of Pd@Pt Core–Shell Ultrathin Nanowires with Enhanced Electrocatalytic Performance toward Oxygen Reduction Reaction. *J. Am. Chem. Soc.* **2015**, *137*, 7862−7868.

(8) Hong, J. W.; Kang, S. W.; Choi, B.-S.; Kim, D.; Lee, S. B.; Han, S. W., Controlled Synthesis of Pd–Pt Alloy Hollow Nanostructures with Enhanced Catalytic Activities for Oxygen Reduction. *ACS Nano* **2012**, *6*, 2410−2419.

(9) Zhou, M.; Wang, H.; Elnabawy, A. O.; Hood, Z. D.; Chi, M.; Xiao, P.; Zhang, Y.; Mavrikakis, M.; Xia, Y., Facile One-Pot Synthesis of Pd@Pt$_{1L}$ Octahedra with Enhanced

Activity and Durability toward Oxygen Reduction. *Chem. Mater.* **2019**, *31*, 1370−1380.

(10) Choi, R.; Choi, S.-I.; Choi, C. H.; Nam, K. M.; Woo, S. I.; Park, J. T.; Han, S. W., Designed Synthesis of Well-Defined Pd@Pt Core–Shell Nanoparticles with Controlled Shell Thickness as Efficient Oxygen Reduction Electrocatalysts. *Chem. Eur. J.* **2013**, *19*, 8190−8198.

(11) Ma, Y.; Yin, L.; Cao, G.; Huang, Q.; He, M.; Wei, W.; Zhao, H.; Zhang, D.; Wang, M.; Yang, T., Pt-Pd Bimetal Popcorn Nanocrystals: Enhancing the Catalytic Performance by Combination Effect of Stable Multipetals Nanostructure and Highly Accessible Active Sites. *Small* **2018**, *14*, 1703613.

(12) Cho, K. Y.; Yeom, Y. S.; Seo, H. Y.; Lee, A. S.; Huy Do, X.; Hong, J. P.; Jeong, H.-K.; Baek, K.-Y.; Yoon, H. G., Fine-sized Pt Nanoparticles Dispersed on PdPt Bimetallic Nanocrystals with Non-covalently Functionalized Graphene toward Synergistic Effects on the Oxygen Reduction Reaction. *Electrochim. Acta* **2017**, *257*, 412−422.

(13) Park, J.; Zhang, L.; Choi, S.-I.; Roling, L. T.; Lu, N.; Herron, J. A.; Xie, S.; Wang, J.; Kim, M. J.; Mavrikakis, M.; Xia, Y., Atomic Layer-by-Layer Deposition of Platinum on Palladium Octahedra for Enhanced Catalysts toward the Oxygen Reduction Reaction. *ACS Nano* **2015**, *9*, 2635−2647.

(14) Xiong, X.; Chen, W.; Wang, W.; Li, J.; Chen, S., Pt-Pd Nanodendrites as Oxygen Reduction Catalyst in Polymer-electrolyte-membrane Fuel Cell. *Int. J. Hydrog. Energy* **2017**, *42*, 25234−25243.

(15) Lee, C.-T.; Wang, H.; Zhao, M.; Yang, T.-H.; Vara, M.; Xia, Y., One-Pot Synthesis of Pd@PtnL Core-Shell Icosahedral Nanocrystals in High Throughput through a Quantitative Analysis of the Reduction Kinetics. *Chem. Eur. J.* **2019,** *25*, 5322−5329.

(16) He, D. S.; He, D.; Wang, J.; Lin, Y.; Yin, P.; Hong, X.; Wu, Y.; Li, Y., Ultrathin Icosahedral Pt-Enriched Nanocage with Excellent Oxygen Reduction Reaction Activity. *J. Am. Chem. Soc.* **2016**, *138*, 1494−1497.

(17) Li, S.; Liu, J.; Zhu, G.; Han, H., Pd@Pt Core–Shell Nanodots Arrays for Efficient Electrocatalytic Oxygen Reduction. *ACS Appl. Nano Mater.* **2019**, *2*, 3695−3700.